View metadata, citation and similar papers at core.ac.uk

brought to you by CORE

provided by Elsevier - Publisher Connector

Cell, Vol. 109, 887–900, June 28, 2002, Copyright ©2002 by Cell Press

MICALs, a Family of Conserved Flavoprotein Oxidoreductases, Function in Plexin-Mediated Axonal Repulsion

Jonathan R. Terman, Tianyi Mao, R. Jeroen Pasterkamp, Hung-Hsiang Yu,[2] and Alex L. Kolodkin[1]
Department of Neuroscience
The Johns Hopkins University School of Medicine
725 North Wolfe Street
Baltimore, Maryland 21205

Summary

Members of the semaphorin family of secreted and transmembrane proteins utilize plexins as neuronal receptors to signal repulsive axon guidance. It remains unknown how plexin proteins are directly linked to the regulation of cytoskeletal dynamics. Here, we show that *Drosophila* MICAL, a large, multidomain, cytosolic protein expressed in axons, interacts with the neuronal plexin A (PlexA) receptor and is required for Semaphorin 1a (Sema-1a)-PlexA-mediated repulsive axon guidance. In addition to containing several domains known to interact with cytoskeletal components, MICAL has a flavoprotein monooxygenase domain, the integrity of which is required for Sema-1a-PlexA repulsive axon guidance. Vertebrate orthologs of *Drosophila* MICAL are neuronally expressed and also interact with vertebrate plexins, and monooxygenase inhibitors abrogate semaphorin-mediated axonal repulsion. These results suggest a novel role for oxidoreductases in repulsive neuronal guidance.

Introduction

During neural development, axons reach their appropriate targets by interpreting a myriad of guidance cues present in their environment. Semaphorin proteins, one of the largest families of guidance cues, are known to influence axon pathfinding, fasciculation, branching, and neuronal cell migration (He et al., 2002; Raper, 2000). A chemorepulsive role in axon guidance has been extensively demonstrated both in vitro and in vivo for many semaphorins, but they also mediate attractive neuronal guidance.

The seven classes of semaphorins include both transmembrane and secreted proteins and are evolutionarily conserved structurally and, in many cases, functionally from invertebrates to vertebrates (Semaphorin Nomenclature Committee, 1999). For example, the transmembrane semaphorin Sema-1a in *Drosophila* is present on developing motor axons and acts as a repellent to regulate motor axon fasciculation in vivo (Yu et al., 1998). The related vertebrate transmembrane semaphorin Sema6A also functions as a repellent for axons of sympathetic neurons in vitro (Xu et al., 2000). Sema3A, a well-characterized vertebrate-secreted semaphorin, is a potent axonal repellent for a variety of neurons in vitro, and in vivo serves as a chemorepellent essential for the establishment of many axonal pathways (Raper, 2000). Similarly, the related *Drosophila*-secreted semaphorin Sema-2a is expressed on developing muscles and regulates motor axon pathfinding as a target-derived chemorepellent (Matthes et al., 1995; Winberg et al., 1998a).

Insight into how semaphorins signal repulsive guidance comes from work showing that plexins, a large family of evolutionarily conserved transmembrane proteins, serve as signal-transducing receptors for both membrane bound and secreted semaphorins (Tamagnone and Comoglio, 2000). The four classes of plexins include proteins that have been found to associate directly with members of five different semaphorin classes. In the *Drosophila* nervous system, plexin A (PlexA) is a functional receptor in vivo for Sema-1a-mediated motor axon repulsion (Winberg et al., 1998b). In vertebrates, repulsion mediated by class 3 secreted semaphorins is dependent on plexin function both in vitro and in vivo (Cheng et al., 2001; reviewed in Tamagnone and Comoglio, 2000). However, repulsive guidance mediated by class 3 semaphorins, including Sema3A and Sema3F, requires a holoreceptor complex that includes a ligand binding obligate coreceptor, neuropilin-1 or neuropilin-2, and a class A plexin. Plexin cytoplasmic domains are highly conserved and, for certain A class plexins, have been shown to be responsible for signaling semaphorin-mediated repulsive axon guidance (Cheng et al., 2001; Takahashi and Strittmatter, 2001).

The repulsive nature of semaphorin signaling mediated by plexin receptors is due to the modification of the growth cone cytoskeleton. For example, following exposure to secreted Sema3A, growth cones undergo rapid collapse, which is accompanied by the depolymerization of F actin and decreased ability to polymerize new F actin (Fan et al., 1993). Several modulators of cytoskeletal dynamics have been implicated in this process including Rho family GTPases, p21-activated kinase (PAK), and LIM kinase (Liu and Strittmatter, 2001; Whitford and Ghosh, 2001). In addition, members of the collapsin response mediator protein (CRMP) family, the Ig superfamily protein L1, intracellular levels of cGMP, and the catalytically inactive receptor tyrosine kinase family member offtrack (OTK) have also been implicated in transducing semaphorin repulsive guidance (He et al., 2002). It remains unknown, however, how plexins directly regulate the activity of these signaling molecules in order to modulate cytoskeletal dynamics.

We show here that a family of flavoprotein monooxygenases, the MICALs, contains members that directly associate with plexins and are required for semaphorin-mediated repulsive axon guidance. Further, MICAL proteins contain multiple domains that are known to be important for interactions with actin, intermediate filaments, and cytoskeletal-associated adaptor proteins. Therefore, MICALs are excellent candidates for directly mediating the cytoskeletal alterations characteristic of

[1]Correspondence: kolodkin@jhmi.edu
[2]Present address: Division of Basic Sciences, Fred Hutchinson Cancer Research Center, 1100 Fairview Ave. N., Seattle, Washington, 98109.

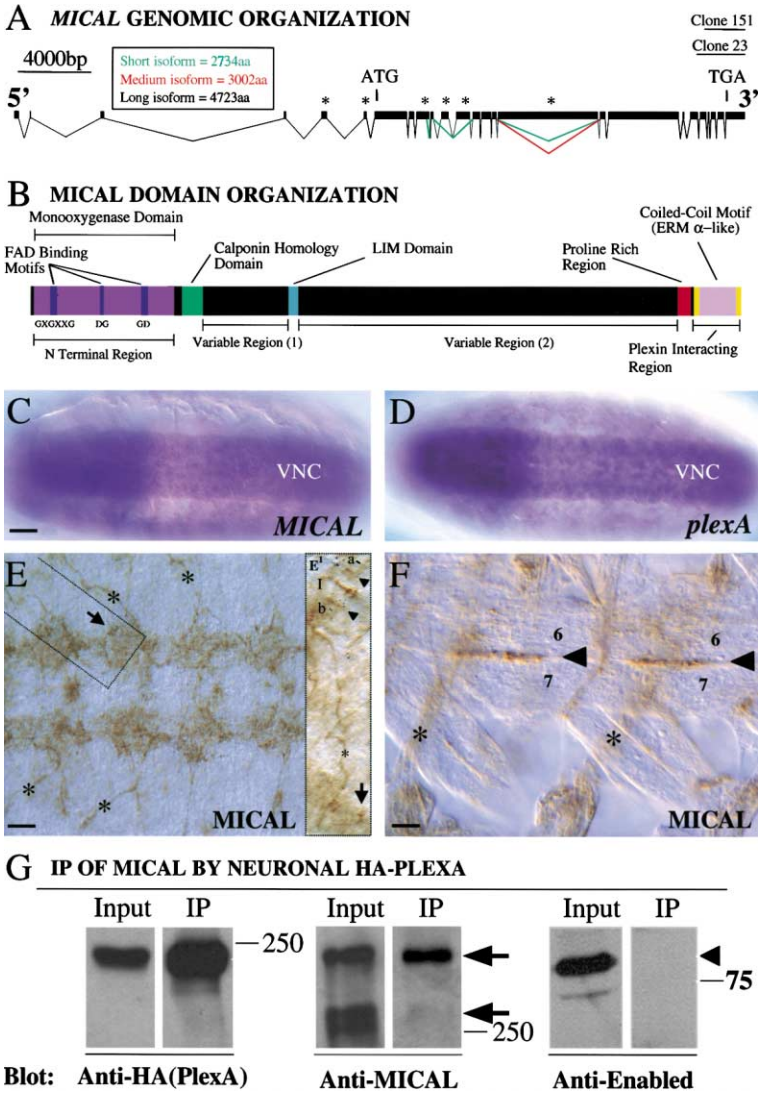

Figure 1. Molecular Characterization of *Drosophila* MICAL, MICAL Expression in *Drosophila* Embryonic Motor Axons, and Coimmunoprecipitation of MICAL with Neuronal PlexA

(A) The *MICAL* locus. Variable exons are indicated with asterisks and produce (1) a "long," (2) a "medium" (spliced out exon is shown in red), and (3) a "short" isoform (spliced out exons shown in green). The regions corresponding to clones 23 and 151 are shown.

(B) MICAL is characterized by flavin adenine dinucleotide (FAD) consensus binding motifs (GXGXXG, DG, and GD motifs), a calponin homology domain, a LIM domain, a proline-rich region, and a coiled-coil motif.

(C and D) Stage 15 whole-mount *Drosophila* embryos following in situ hybridization with antisense probes to *MICAL* (A) and *PlexA* (B). Anterior to left. Ventral nerve cord (VNC).

(E and F) Filleted stage 15/16 *Drosophila* embryos immunostained with MICAL antiserum (anterior is to the left). The region outlined in (E) is shown in higher power in (E^1) from a similarly staged embryo. MICAL decorates motor neuron cell bodies (arrows) and their bundled axons (asterisks) as they exit the ventral nerve cord and innervate their muscle targets (arrowheads). Abbreviations: 6, 7, muscles 6 and 7; I, ISN; b, ISNb; and a, SNa.

(G) MICAL and PlexA proteins associate in *Drosophila* neurons in vivo. Embryonic lysates derived from embryos with neuronally expressed HA-PlexA(input) were immunoprecipitated (IP) using HA antibodies and immunoblotted with antibodies directed against HA (left), MICAL (middle), or Enabled (right). Robust coimmunoprecipitation of MICAL (arrows), but not Ena (arrowhead), is observed with HA (PlexA) antibodies. Molecular weight is in kilodaltons. Scale bar equals 30 μm (C and D); 18 μm (E); 12 μm (F).

semaphorin signaling and provide novel targets for the attenuation of axonal repulsion.

Results

MICAL Is a Large, Cytosolic, Multidomain Protein that Interacts with *Drosophila* Plexin A

To identify mediators of semaphorin-dependent repulsive axonal guidance, we used the terminal highly conserved "C2" portion of the PlexA cytoplasmic domain to search for interacting proteins encoded by a *Drosophila* embryonic (0–24 hr) yeast two-hybrid cDNA library (see Supplemental Figures S1A–S1C at http://www.cell.com/cgi/content/full/109/7/887/DC1). Although the strongest interactors we identified (clones 151 and 23) (Figure 1A) interacted with PlexA in yeast, they did not interact with the C2 region of the other *Drosophila* plexin, PlexB (see Supplemental Figure S1B). Extensive molecular analysis demonstrated that the *Drosophila* gene defined by clones 23 and 151, which we have called *MICAL* (see below), covers >41 kb of genomic sequence and has at least 25 exons (Figure 1A; see Supplemental Figure S1). Based on analysis of isolated cDNAs and Western analysis (see Supplemental Figure S2D), there are at least three MICAL isoforms ("long," "medium," and "short" variants; Figure 1A).

Drosophila MICAL is named for its recently characterized vertebrate ortholog, MICAL-1 (for *m*olecule *i*nteracting with *CasL*), which has been shown to associate with CasL and vimentin in nonneuronal cells (Suzuki et al., 2002). Within the plexin-interacting region in the C terminus identified in our screen, there is a predicted heptad-repeat, coiled-coil structure (Figure 1B; data not shown). Interestingly, this region of MICAL shares amino acid similarity with several other coiled-coil domain-containing proteins including a portion of the α domain found in the *E*zrin, *R*adixin, and *M*oesin (ERM) proteins (~22% identity; data not shown; Bretscher et al., 2000). N-terminal to this domain there is a region rich in prolines, and the last four amino acids of MICAL (ESII) are a PDZ protein binding motif (Harris and Lim, 2001). There are two regions of varying length, with no significant similarity to other proteins, which appear to determine the size of the different MICAL proteins (Figure 1B).

MICAL has a single LIM domain (Figure 1B; data not shown), a protein-protein interaction module found in a variety of proteins involved in signal transduction cascades and in cytoskeletal organization (Bach, 2000), and also a single calponin homology (CH) domain (Figure1B; data not shown), a domain also found in cytoskeletal and signal transduction proteins and known to be involved in actin filament binding (Gimona et al., 2002). The MICAL N-terminal ~500 aa is highly conserved among MICAL-related proteins (see below) but is unique over its entire length in comparison to other proteins.

MICAL Is Expressed on *Drosophila* Embryonic Motor and CNS Axons and Coimmunoprecipitates with PlexA

In situ hybridization analysis using RNA probes corresponding to the N or C terminus of MICAL shows that *MICAL* and *PlexA* have similar patterns of embryonic mRNA expression. During early *Drosophila* development (stages 7–8), both are expressed in the ventral neurogenic region and in many nonneuronal tissues (including developing mesoderm, cells surrounding the cephalic furrow and amnioproctodeal invagination, and in gut primordia). This nonneuronal expression is also seen later in embryonic development (stages 11–17), where both are present within the anterior and posterior midgut primordia, the visceral musculature, and weakly in somatic musculature. During axonal pathfinding (stage 13 onward), both are expressed within the developing brain and ventral nerve cord in most, if not all, CNS neurons (Figures 1C and 1D; data not shown), but *MICAL*, like *Sema1a* and *PlexA*, is not highly expressed in peripheral sensory neurons.

Western blot analysis using a polyclonal antibody directed against the MICAL C terminus (MICAL-CT) revealed prominent bands at 530 kDa, 330 kDa, 300 kDa, 200 kDa, and 125 kDa in lysates from wild-type embryos which increase in intensity in lysates from embryos harboring a chromosomal duplication that includes the MICAL locus (see Supplemental Figure S2D at http://www.cell.com/cgi/content/full/109/7/887/DC1). The three largest protein bands correspond to the predicted molecular weights of the three MICAL cDNAs (Figures 1A). These bands were not present in embryonic lysates obtained from embryos harboring a deficiency that includes the *MICAL* locus (see below and Supplemental Figure S2D).

MICAL protein is present in neuronal cell bodies, along axons, and in growth cones (Figures 1E and 1F; data not shown). MICAL immunostaining first appears in the nervous system at stage 13 and labels motor and CNS projections, and at later embryonic stages, it is present on axons that make up all motor axon pathways: the intersegmental nerve (ISN), the intersegmental nerves b and d (ISNb and ISNd), and the segmental nerves a and c (SNa and SNc) (Figures 2E and 2F; data not shown). MICAL immunostaining is also present in segment boundaries at the position of muscle attachment sites and at low levels in the lateral cluster of chordotonal organs.

To ask whether PlexA and MICAL directly interact in neurons, we generated flies that contain a transgene encoding epitope-tagged PlexA (HA-PlexA) under the control of an upstream activator sequence (UAS) (Brand and Perrimon, 1993) and crossed them to flies that express the GAL4 transcription factor in all neurons (*Elav-GAL4*). In lysates from the resulting embryos, we observed robust coimmunoprecipitation of MICAL using HA antibodies (Figure 1G) and also reciprocal coimmunoprecipitation of HA-PlexA using MICAL-CT antibodies (data not shown). The "large" MICAL isoform is the predominant variant observed to be associated with neuronally expressed HA-PlexA, which may reflect tissue-specific expression of this isoform in neurons. MICAL coimmunoprecipitation appears specific since enabled (Ena), a neuronally expressed cytosolic protein, was not coimmunoprecipitated by HA antibodies in similar experiments (Figure 1G), and Unc5, a neuronally expressed transmembrane receptor, was not coimmunoprecipitated by MICAL-CT antibodies (data not shown).

A *MICAL* Loss-of-Function Mutant Demonstrates that MICAL Is Required for Motor Axon Pathfinding

To determine whether MICAL functions in vivo to propagate Sema-1a-mediated motor axon guidance, we performed detailed genetic analyses of *MICAL* gain- and loss-of-function mutants. We generated a small, tractable deficiency (called $Df(3R)swp2^{MICAL}$; see Supplemental Figure S2 at http://www.cell.com/cgi/content/full/109/7/887/DC1) that removes ~170 kb that includes the *MICAL* locus and ~6 other genes. Western blot analysis on lysates from embryos homozygous for $Df(3R)swp2^{MICAL}$ demonstrates a loss of all MICAL protein (Supplemental Figure S2D), and no MICAL immunostaining is observed in these embryos (data not shown). These data, in combination with rescue experiments using a *MICAL* cDNA (see below), define the small deficiency $Df(3R)swp2^{MICAL}$ as a *MICAL* null allele. $Df(3R)swp2^{MICAL}$ homozygotes survive into larval stages and have no overt morphological abnormalities (see Supplemental Figure S2).

If MICAL functions in Sema-1a/PlexA-dependent repulsive axon guidance, then *MICAL* LOF mutants should exhibit motor axon guidance defects similar to the distinct and highly penetrant defects seen in *Sema1a* and *PlexA* LOF mutants. The development of the stereotypic pattern of neuromuscular connectivity in embryonic *Drosophila* abdominal segments is observed with anti-fasciclin II (mAb 1D4) staining of stage 16/17 embryos (VanVactor et al., 1993). Motor axons initially exit the CNS as part of either the intersegmental nerve (ISN) or the segmental nerve (SN). They are then guided into five major nerve branches (the ISN, ISNb, ISNd, SNa, and SNc), each of which targets different muscle groups such that individual motor axons eventually innervate individual target muscles (Landgraf et al., 1997).

In wild-type embryos, the ISNb is formed by ISN axons defasciculating and extending dorsally through the ventral musculature to innervate muscles 6 and 7 and muscles 12 and 13 (Figures 2A and 4E). Axons within the ISNb pathway in *Sema1a* or *PlexA* mutants often fail to defasciculate and innervate their muscle targets (Figure 2B; Table 1; Winberg et al., 1998b; Yu et al., 1998). In the absence of *MICAL*, axons within the ISNb show similar highly penetrant ISNb phenotypes (Figure 2C; Table 1). These phenotypes include the failure of some

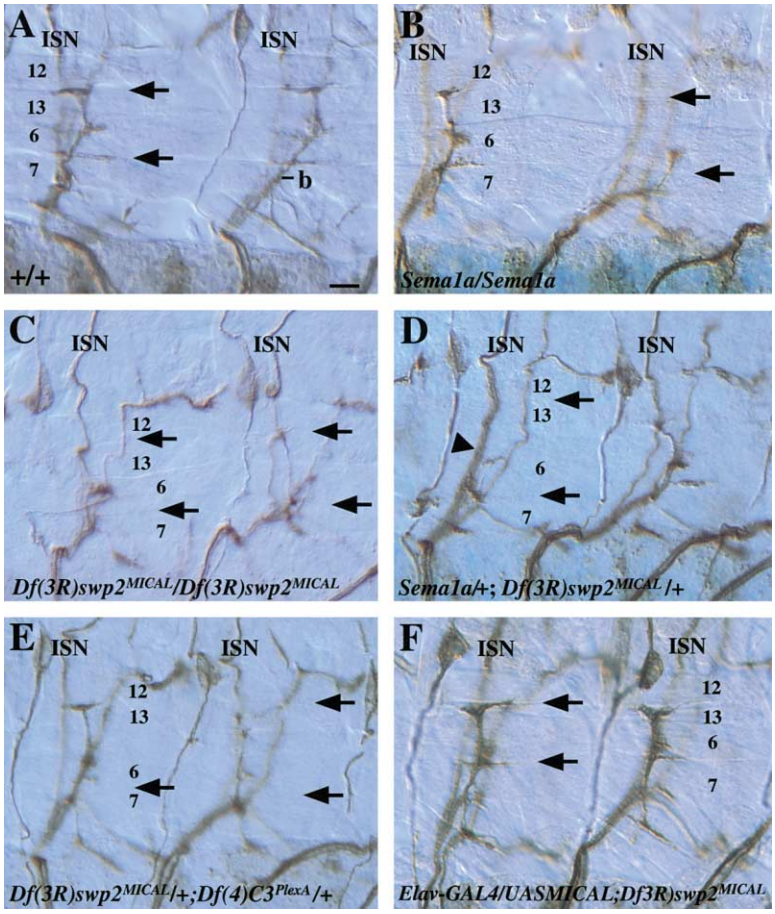

Figure 2. *MICAL* Is Required for ISNb Pathway Formation and Interacts Genetically with *Sema1a* and *PlexA*

Abdominal segments of filleted stage 16/17 embryos stained with mAb 1D4 to reveal motor axons. Ventral muscles 6, 7, 12, and 13 and the intersegmental nerve (ISN) are labeled. Anterior, left; dorsal, up.

(A) Axons comprising the ISNb (b) in a wild-type embryo defasciculate from the ISN and grow dorsally through the ventral musculature to innervate muscles 6/7 and muscles 12/13 (arrows).

(B) Axons within the ISNb of a *Sema1a* mutant embryo often fail to innervate muscles 6/7 and 12/13 (arrows).

(C) Axons within the ISNb of a homozygous *MICAL* mutant (Df(3R)swp2^{MICAL}) fail to innervate muscles 6/7 and 12/13 (arrows). In the left hemisegment, some axons bypass muscles 6/7 and then stall prior to reaching muscles 12/13.

(D and E) *MICAL* interacts genetically with *Sema1a* and *PlexA*. Axons within the ISNb of an embryo transheterozygous for *MICAL* and *sema1a* (*sema1a*/+;*Df(3R)swp2*^{MICAL}/+) or *MICAL* and *PlexA* (*Df(3R)swp2*^{MICAL}/+; *Df(4)C3*^{PlexA}/+) often fail to innervate muscles 6/7 and 12/13 (arrows). Some ISNb axons fail to defasciculate from the ISN and exhibit a bypass phenotype (arrowhead, [D]).

(F) Expression of MICAL in all neurons rescues the ISNb defects observed in *MICAL* mutant embryos. Axons within the ISNb innervate muscles 6/7 and 12/13 normally (e.g., arrows). Scale bar equals 16 μm and can be applied to Figures 3 and 4.

or all axons to defasciculate from the ISN, stalling of axons within the ISNb following defasciculation from the ISN, ISNb axons bypassing their target muscle groups, and greatly reduced or absent innervation of target muscles.

Axons within the SNa pathway in *MICAL* mutants also exhibit highly penetrant defects similar to those observed in both *Sema1a* mutants and *PlexA* mutants. In wild-type embryos, SNa axons defasciculate from the SN and extend through the ventral musculature as a single tightly fasciculated bundle (Figure 3A). At the dorsal edge of muscle 12, SNa axons defasciculate to give rise to a dorsal (D) and lateral (L) branch. Axons within the dorsal branch extend dorsally between muscles 22 and 23 and then make two characteristic turns, continuing farther dorsally between muscles 23 and 24 (Figures 3A and 4E). In *Sema1a* and *PlexA* mutants, SNa axons within the dorsal branch often stall near muscle 12 and fail to reach the dorsal-most portion of their trajectory (Figure 3B; Table 1; Winberg et al., 1998b; Yu et al., 1998). *MICAL* mutants exhibit similar, highly penetrant, SNa stall phenotypes (Figures 3C; Table 1). *MICAL* mutants also exhibit prominent guidance defects in axons that give rise to the ISNd, SNc, TN, and the third most lateral fasciclin II—positive CNS longitudinal connective (Figure 2C; data not shown)—defects that have been observed in *Sema1a* and *PlexA* mutants (Winberg et al., 1998b; Yu et al., 1998; data not shown). In *MICAL* LOF mutant embryos, we did not see additional phenotypes beyond those seen in *PlexA* and *Sema1a* mutants, suggesting that MICAL primarily functions during *Drosophila* neural development in PlexA signaling events.

We restored *MICAL* expression in homozygous *Df(3R)swp2*^{MICAL} embryos using one copy of the transgenic construct *UAS-MICAL* under the control of the neuron-specific driver *Elav-GAL4*. Due to the large size of the MICAL protein, we attempted our rescue using the smallest MICAL isoform—the 300 kDa "small" form (Figure 1A). The level of neuronal MICAL expression observed by immunostaining with MICAL antibodies in three independent MICAL transformants was somewhat lower than wild-type levels (data not shown). Neuronal *MICAL* expression did not rescue the adult lethality in *Df(3R)swp2*^{MICAL} homozygotes, suggesting a requirement for the MICAL "long" form, other genes within the *Df(3R)swp2*^{MICAL} deficiency, and/or MICAL in nonneuronal cells for adult viability. We did, however, observe that neuronal *MICAL* expression in homozygous *Df(3R)swp2*^{MICAL} embryos almost completely rescues embryonic ISNb and SNa motor axon guidance defects (Table 1; Figures 2F, 3F, and 4E) and CNS longitudinal connective defects (data not shown). Therefore, axon guidance phenotypes observed in the *MICAL* deficiency *Df(3R)swp2*^{MICAL} result from a lack of neuronal MICAL.

MICAL Genetically Interacts with *Sema1a* and *PlexA*

To address whether MICAL functions in the same signaling pathway with PlexA to mediate Sema-1a-mediated

Table 1. Axon Guidance Phenotypes (ISNb and SNa Phenotypes)

Genotype (Hemisegments)	Abnormal ISNb Bypass[a]([x])	Abnormal Muscle 6/7 Innervation[b]([y])	Abnormal Muscle 12/13 Innervation[b]	SNa Pathway[c]([z])
Controls				
+/+ (wild type) (n = 120)	0%	1.7%	2.5%	10.0%
Elav-GAL4/+ (n = 130)	0% (0%)	1.5% (0%)	4.6%	8.5% (0%)
Elav-GAL4/Elav-GAL4 (n = 109)	0% (0%)	2.8 (0%)	8.2%	12.8% (0%)
Df(3R)swp2^{MICAL}/+ (n = 110)	0%	3.6%	7.2%	7.3%
Sema1a^{P1}/+ (n = 110)	0%	2.7%	8.1%	9.1%
Df(4)C3^{PlexA}/+ (n = 101)	0%	1.0%	3.0%	12.0%
Loss of Function				
Df(3R)swp2^{MICAL}/Df(3R)swp2^{MICAL} (n = 103)	1.0%	68.9%	57.3%	81.2%
Sema1a^{P1}/Sema1a^{P1} (n = 97)	5.2%	47.4%	77.3%	85.7%
Df(4)C3^{PlexA}/Df(4)C3^{PlexA} (n = 148)	4.1%	60.8%	47.3%	74.3%
Elav-GAL4/UASMICAL; Df(3R)swp2^{MICAL}/*Df(3R)swp2^{MICAL}* (n = 138)	0%	5.8%	13.0%	20.3%
UASMICAL$^{G\rightarrow W}$/+; *Elav-GAL 4*/+; *Df(3R)sup2^{MICAL}/Df(3R)swp2^{MICAL}* (n = 137)	0%	67.2%	68.6%	69.7%
Genetic Interactions				
Sema1a^{P1}/+;*Df(3R)swp2^{MICAL}*/+ (n = 110)	3.6%	32.7%	37.3%	51.8%
Df(3R)swp2^{MICAL}/+;*Df(4)C3^{PlexA}*/+ (n = 105)	0%	41.9%	33.0%	44.6%
Sema1a^{P1}/+;*Df(4)C3^{PlexA}*/+ (n = 108)	0%	32.4%	39.8%	68.5%
Sema1a^{P1},*Elav-GAL4*/+; *UASMICAL/Df(3R)swp2^{MICAL}* (n = 99)	0%	6.1%	6.1%	9.2%
Gain of Function				
Elav-GAL4/Elav-GAL4; *UASMICAL$^{Myr\text{-}CT}$/UASMICAL$^{Myr\text{-}CT}$* (n = 97)	2.1% (50%)	32.0% (3.2%)	48.5%	46.4% (2.2%)
UASMICAL/UASMICAL; Elav-GAL4/Elav-GAL4 (n = 130)	0.8% (100%)	44.2% (59.6%)	50.0%	38.0% (71.4%)
UASMICAL$^{G\rightarrow W}$/+; *Elav-GAL4*/+ (n = 170)	2.4% (100%)	36.7% (43.5%)	44.4%	48.5% (37.8%)

Description of phenotypes is as follows (x, y, and z indicate percent of defects in a, b, and c, respectively).
[a] Failure of all ISNb axons to defasciculate from the ISN.
[b] ISNb axons stalling, bypassing targets, absent or decreased muscle innervation.
[c] Failure to make the two characteristic turns between muscles 22 and 23 and muscles 23 and 24.
[x] All ISNb axons follow the ISNd or SNc, or ISNb axons remain fasciculated with the ISN but ultimately wander in the lateral muscle fields or project back to innervate ventral muscles.
[y] Increased (long or excessively thick) muscle innervation, excessive branching, or projecting into abnormal target fields.
[z] Fasciculation with the ISN, premature branching, following abnormal pathways, or termination on wrong muscles.

repulsive axon guidance, we employed classical genetic interaction analysis by asking whether heterozygosity at both *MICAL* and *PlexA*, or *MICAL* and *Sema1a*, resulted in phenotypes not observed in either heterozygote alone. *MICAL*, *PlexA*, or *Sema1a* heterozygous embryos show no motor axon guidance defects (Table 1). Embryos heterozygous for both *Sema1a* and *PlexA* (*Sema1a/+;Df(4)C3^{PlexA}/+*) show highly penetrant axon guidance defects similar to those observed in homozygous *Sema1a* or *PlexA* mutants (Table 1; Winberg et al., 1998b). Embryos heterozygous for both *MICAL* and *Sema1a*, or heterozygous for both *MICAL* and *PlexA*, exhibit axon guidance phenotypes similar to those seen in *Sema1a/+;Df(4)C3^{PlexA}/+* embryos, and these are seen at approximately equal penetrance (Table 1). For example, the ISNb and SNa of *Sema1a/+;Df(3R)swp2^{MICAL}/+* or *Df(3R)swp2^{MICAL}/+;Df(4)C3^{PlexA}/+* embryos exhibit guidance errors at specific choice points similar to those seen in homozygous *PlexA*, *Sema1a*, or *MICAL* mutant embryos (Figures 2D, 2E, 3D, 3E, and 4E). We reintroduced one copy each of both the *UAS-MICAL* and *Elav-GAL4* transgenes into the *Sema1a/+;Df(3R)swp2^{MICAL}/+* background and observed that neuronal *MICAL* expression rescues both the ISNb and SNa phenotypes in these transheterozygous embryos (Table 1). These results support the idea that MICAL and PlexA function in the same signaling pathway to guide motor axons.

MICAL Gain-Of-Function Axon Guidance Phenotypes

To complement *MICAL* LOF analysis, we asked whether *MICAL* GOF mutants exhibit motor axon guidance phenotypes similar to those observed in *PlexA* GOF mutants (Winberg et al., 1998b). We overexpressed MICAL in all neurons in a wild-type background using the GAL4-UAS system, and one or two copies of our *MICAL* rescue construct leads to highly penetrant motor axon guidance phenotypes (Table 1; data not shown). GOF phenotypes resulting from one copy of the *MICAL* rescue construct in a wild-type background can be suppressed in a *Df(3R)swp2^{MICAL}* genetic background (Table 1; data not shown). GOF defects in some cases are quite similar to the defects we observe in *MICAL* mutants and defects reported in *PlexA* GOF mutants (Winberg et al., 1998b).

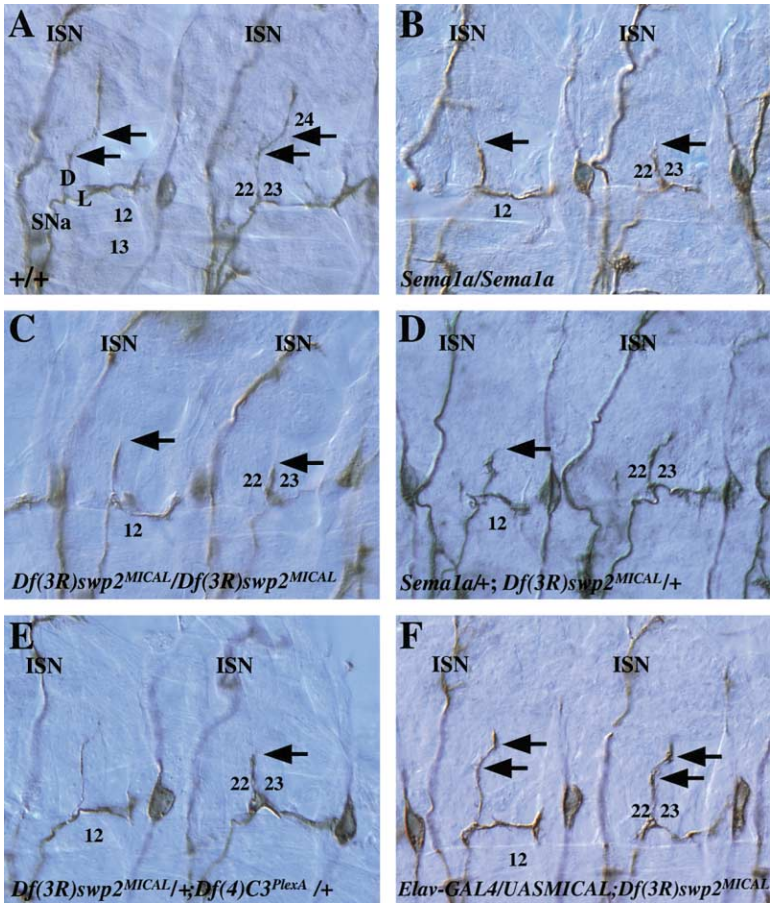

Figure 3. *MICAL* Is Required for Proper Formation of the SNa Pathway and Interacts Genetically with *Sema1a* and *PlexA*

Abdominal segments of filleted stage 16/17 embryos stained as in Figure 2. Ventral muscles 12 and 13 and lateral muscles 22, 23, and 24 are labeled. Anterior, left; dorsal, up.

(A) Axons that make up the SNa in a wild-type embryo extend through the ventral musculature as a fasciculated bundle (SNa). After reaching the dorsal edge of muscle 12, axons within the SNa give rise to a dorsal (D) and lateral (caudal) (L) branch. Axons within the dorsal branch extend dorsally between muscles 22 and 23 and then make two characteristic turns (arrows) and continue extending dorsally between muscles 23 and 24.

(B) Axons within the SNa of a *Sema1a* mutant embryo fail to make the two characteristic turns and instead stall just dorsal to muscle 12 between muscles 22 and 23 (arrows).

(C) Axons within the SNa of a *MICAL* mutant (*Df(3R)swp2*^{MICAL}) stall just dorsal to muscle 12 (arrows).

(D and E) *MICAL* interacts genetically with *Sema1a* and *PlexA*. Axons within the SNa of an embryo transheterozygous for *MICAL* and *Sema1a* (*sema1a/+;Df(3R)swp2*^{MICAL}*/+*) (D) or *MICAL* and *PlexA* (*Df(3R)swp2*^{MICAL}*/+; Df(4)C3*^{PlexA}*/+*) (E) often fail to reach their dorsal targets (arrows).

(F) Expression of MICAL in all neurons rescues the SNa pathfinding defects observed in *MICAL* mutant embryos. Axons within the SNa project normally to their dorsal muscle targets, making both characteristic turns (arrows).

However, a large fraction of these *MICAL* GOF motor axon guidance phenotypes are consistent with increased defasciculation (Table 1), as similarly described for the *PlexA* GOF mutants. For example, ISNb axons were often seen to abnormally leave the ISNb and project incorrectly within the ventral musculature (Figures 4A and 4E; Table 1). Likewise, some SNa axons defasciculated at incorrect locations and projected to inappropriate areas (Figure 4B; Table 1). Therefore, MICAL GOF mutants exhibit phenotypes similar to *PlexA* GOF mutants (Figure 4E), again suggesting that MICAL participates in PlexA-mediated motor axon guidance.

Additional support for MICAL's role in PlexA signaling was obtained by expressing in all neurons a truncated *MICAL* protein consisting only of the MICAL PlexA-interacting region (Figure 1B). We targeted this protein to the cell membrane by introducing an N-terminal myristoylation sequence (MICAL$^{Myr\text{-}CT}$) and found that neuronally expressed MICAL$^{Myr\text{-}CT}$ acts in a dominant-negative fashion, resulting in axon guidance phenotypes similar to those observed in *MICAL* mutants (Figures 4C–4E; Table 1; data not shown). We did not observe prominent GOF phenotypes like those resulting from MICAL or PlexA overexpression (Table1), indicating that neuronal MICAL$^{Myr\text{-}CT}$ is likely occluding normal MICAL-PlexA associations and therefore MICAL signaling. This also suggests that the MICAL protein contains domains distinct from the PlexA-interacting domain that function to regulate axonal guidance.

The MICALs Are a Family of Neuronally Expressed, Plexin-Interacting Proteins Conserved from Flies to Mammals

MICAL proteins have conserved protein domains with identical organization in all family members and a high degree of amino acid identity among these domains in different MICALs (Figure 5A). Suzuki et al. (2002) identified MICAL-1 and a partial sequence of MICAL-2. We have found that there is one MICAL in *Drosophila* and three mammalian MICALs. The MICALs appear unique with respect to containing both calponin homology (CH) and LIM domains, in addition to their conserved N- and C-terminal regions. We have also found a family of MICAL-like (MICAL-L) proteins, members of which have a similar organization to MICALs but lack the region N-terminal to the CH domain (Figure 5B). There is one MICAL-L protein in *Drosophila* (D-MICAL-L) and at least two family members in humans. *D-MICAL-L* cDNA and genomic DNA sequence information suggest that D-MICAL-L begins just N-terminal to the CH domain. Analysis of publicly available mammalian cDNA and genomic sequences suggests that human MICAL-L1 and MICAL-L2 are similar in overall domain organization to D-MICAL-L and do not contain the highly conserved ~500 aa MICAL N-terminal domain.

To address whether the function of MICALs is conserved in vertebrates, we looked at expression patterns and interactions with plexins and found that the mRNA of all three rat *MICALs* shows specific neuronal and

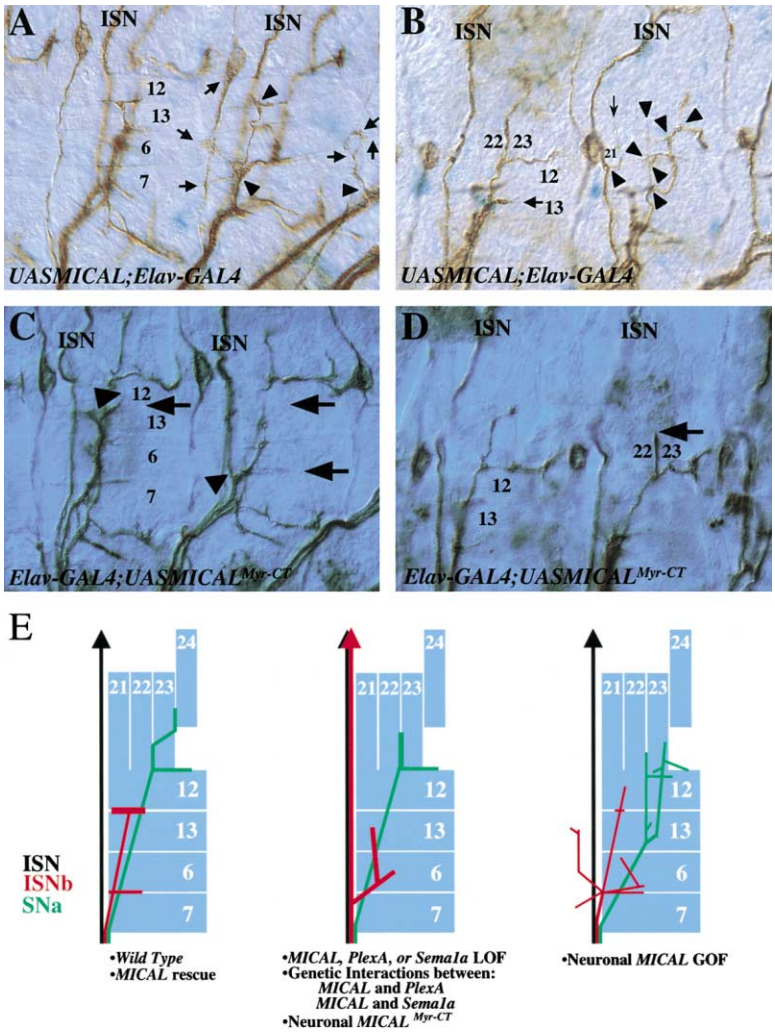

Figure 4. *MICAL* Gain-Of-Function Axon Guidance Phenotypes

Abdominal segments of filleted stage 16/17 embryos stained as in Figure 2.

(A and B) MICAL overexpression in all neurons in a wild-type background using the GAL4-UAS system leads to GOF motor axon guidance phenotypes including increased defasciculation of axons of the ISNb and SNa. Axons were often seen exiting their nerve prematurely or abnormally (arrowheads) and projecting inappropriately (e.g., arrows). Abnormal pathfinding by SNa axons or inappropriate innervation of muscle 21 by axons within the ISN was also observed (thin arrow, [B]).

(C and D) Embryos expressing MICAL$^{Myr\text{-}CT}$ in all neurons using the GAL4-UAS system exhibit motor axon guidance phenotypes similar to those observed in MICAL loss-of-function mutants. Axons within the ISNb fail to properly innervate muscles 6/7 and 12/13 (arrows, [C]), and axons within the SNa fail to make their two characteristic turns and reach their dorsal muscle targets (arrow, [D]). In these segments, some ISNb axons (C) are seen to bypass their muscle targets (arrowheads, [C]).

(E) Schematic representation of *MICAL* genetic analysis and motor axon phenotypes (see text).

nonneuronal expression during development (Figures 5C–5H; data not shown). For example, *MICAL1, MICAL2,* and *MICAL3* are expressed in the rat spinal cord, dorsal root ganglia (DRG), and sympathetic ganglia at embryonic days 15 (E15) and E18 in patterns that appear overlapping but distinct (Figures 5C–5H). Interestingly, the neuronal expression patterns of individual *MICALs* are similar to those observed for several plexins, as can be seen for *PlexA3* and *MICAL1* (Figures 5F and 5I; data not shown). In addition, our results to date indicate that the plexin-interacting domains of human MICAL-1 and mouse MICAL-2 specifically interact with the C2 domains of human PlexA3 and mouse PlexA4, respectively, and do so as strongly as the orthologous domains of *Drosophila* MICAL and PlexA (see Supplemental Figure S1B at http://www.cell.com/cgi/content/full/109/7/887/DC1).

MICALs Contain an N-Terminal Flavoprotein Monooxygenase Domain

The high degree of conservation of the MICAL N terminus among family members (up to 62% identical between flies and humans) (Figure 5A) suggests that this domain is functionally important. Upon closer examination of the 500 aa conserved N-terminal region, we noted a consensus dinucleotide binding sequence, GXGXXG (Figures 1B and 6A), which is distinct from the sequence present in classical mononucleotide binding motifs (Eggink et al., 1990; Eppink et al., 1997; Schulz, 1992; Wierenga et al., 1986). Further, this region contains three separate motifs found in flavoprotein monooxygenases (also called hydroxylases), a subclass of oxidoreductases (Eggink et al., 1990; Eppink et al., 1997; Wierenga et al., 1986). The amino acid sequence surrounding the GXGXXG motif matches perfectly the consensus sequence for the ADP binding region of flavin adenine dinucleotide (FAD) binding proteins (Rossmann fold or FAD fingerprint 1) (Figures 1B and 6A), and distinguishes this region from consensus NAD, or NADP binding folds (Vallon, 2000; Wierenga et al., 1986). MICALs also have a well-conserved GD motif (FAD fingerprint 2) (Figures 1B and 6A) C-terminal to the FAD fingerprint 1 region, which is important for binding the ribose moiety of FAD (Eggink et al., 1990; Eppink et al., 1997). Finally, MICALs have the conserved DG motif ("conserved motif"; Figures 1B and 6A) between the FAD fingerprint 1 and 2 motifs that has been reported to be involved in binding the pyrophosphate moiety of FAD (Eppink et al., 1997).

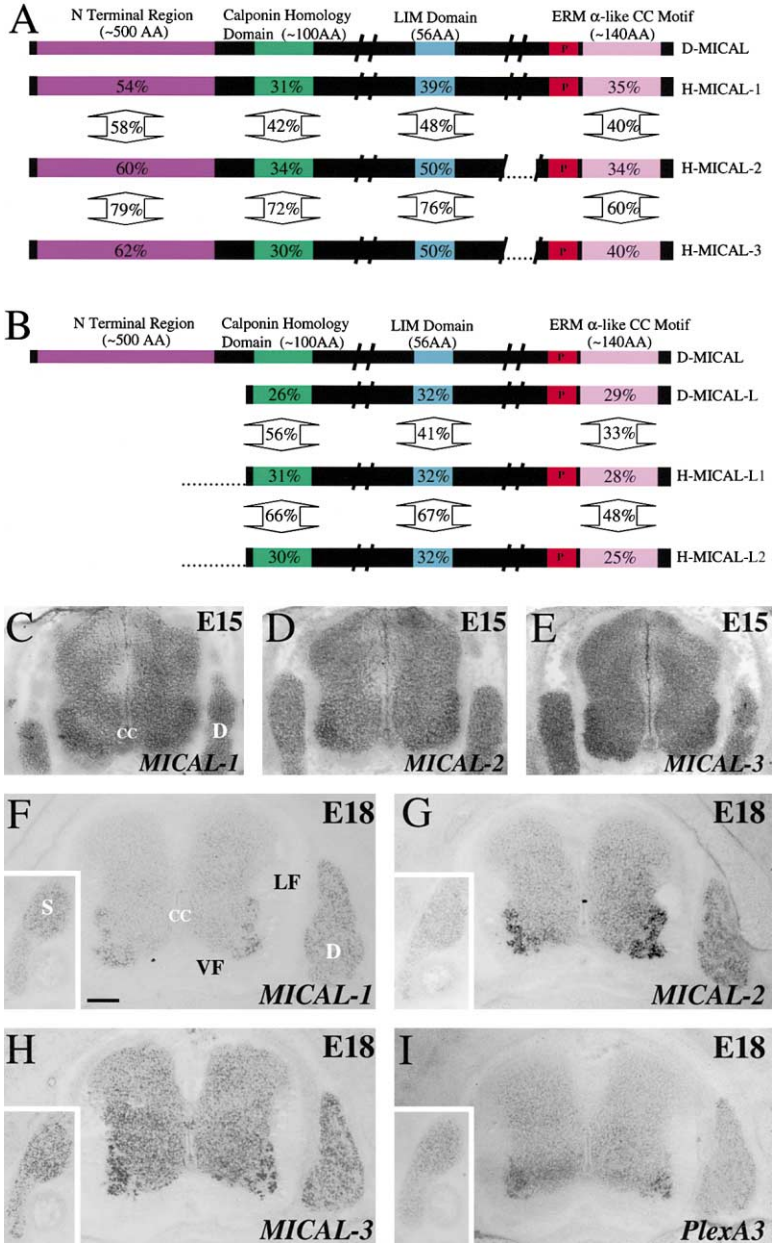

Figure 5. The MICALs Are a Family of Neuronally Expressed Plexin-Interacting Proteins Conserved from Flies to Mammals

(A) The MICAL family of proteins. Amino acid identities are indicated among vertebrate MICALs and *Drosophila* MICAL (percents within domains) and between vertebrate MICALs (percents in arrows). The black regions indicate sequences that are not well conserved among family members and variable in length (//). Regions encoded by an ORF situated in close proximity in the genome (~10 kb) but for which cDNA sequence connecting them has not yet been identified are indicated (dots).

(B) MICAL-like proteins have a similar domain organization as the MICALs but lack the N-terminal ~500 aa domain. Domain alignment and amino acid identity between *Drosophila* MICAL and MICAL-like proteins is indicated (within domains) and between MICAL-like proteins (within arrows). Available *D-MICAL-L* cDNA and genomic DNA sequence information suggests that the D-MICAL-L protein begins just N-terminal to the CH domain. Human MICAL-L1 and MICAL-L2 are similar in overall domain organization to D-MICAL-L and do not contain the highly conserved ~500 aa MICAL N-terminal domain (dots indicate where molecular analysis is required to conclusively define the structural features of mammalian MICAL-L proteins). Abbreviations: P, proline-rich region; cc, coiled-coil.

(C–H) *MICAL* family members are expressed in the developing vertebrate nervous system. Photomicrographs of adjacent sections through the thoracic level of the E15 (C–E) and E18 rat (F–H) spinal cord and dorsal root ganglia (D) following in situ hybridization with antisense probes specific for each *MICAL* are shown. The insets (F–H) show E18 *MICAL* expression in sympathetic ganglia (S) at the same axial level. *MICAL*s are expressed in what appear to be overlapping but distinct patterns.

(I) *plexin A3* is expressed in a pattern similar to *MICAL-1*, seen here in sections adjacent to those in (F)–(H) following in situ hybridization with antisense probes specific for *plexin A3*. Abbreviations: VF, ventral funiculus; LF, lateral funiculus; and CC, central canal. Scale bar equals 150 μm (C–E); 225 μm (F–I).

Proteins with these consensus FAD binding regions use FAD in the catalysis of oxidation-reduction reactions. Flavoprotein monooxygenases are oxidoreductases (enzymes that catalyze oxidation and reduction reactions) that catalyze the insertion of one atom of molecular oxygen into their substrate using nucleotides as electron donors (Massey, 1995). These monooxygenases are also defined by their use of FAD as a coenzyme. Apart from these three consensus regions, monooxygenases vary significantly, reflecting the wide range of enzymes in this family and their variable substrate binding pockets also encompassed within this domain (Eppink et al., 1997). However, MICALs and other monooxygenases show significant similarity within these three FAD binding regions and also similar spacing of these regions within the monooxygenase domain.

To ask whether MICAL binds FAD, we made a bacterial fusion protein containing the MICAL flavoprotein monooxygenase domain (MICAL-FM). A solution of the purified MICAL-FM is yellow in color, a characteristic of flavoproteins. Spectral analysis of purified MICAL-FM shows that it has an absorption peak at 452 nm and a shoulder at ~358 nm (Figure 6B). This is similar to the absorption spectra of FAD itself (~450 nm and ~360 nm; Macheroux, 1999) and to other related flavoproteins (e.g., *p*-hydroxybenzoate hydroxylase [Hosokawa and Stanier, 1966] and GidA [White et al., 2001]), suggesting that MICAL-FM binds FAD. These results, in combination with the sequence homology, raise the possibility that MICAL enzymatic activity within the N-terminal conserved domain serves an integral function in plexin signaling.

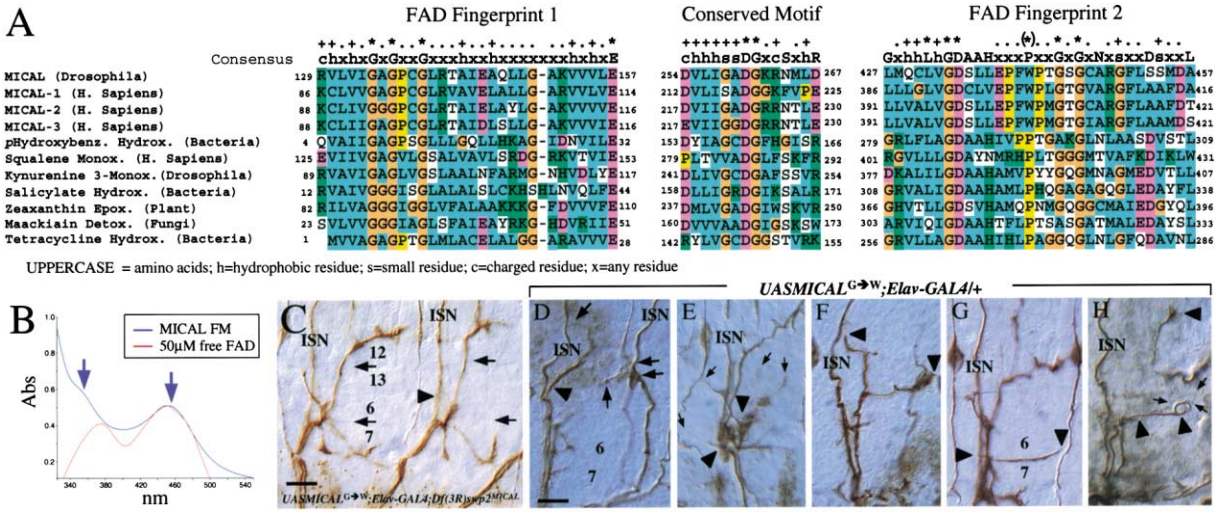

Figure 6. The MICALs Contain Flavoprotein Monooxygenase Domains Required for MICAL Function in *Drosophila*

(A) MICALs contain three sequence motifs that define them as flavoprotein monooxygenases. An alignment of MICALs with members of the flavoprotein monooxygenase family is shown in which a plus sign indicates that MICALs match the consensus, an asterisk indicates that MICALs match the highly important conserved residues, and a dot indicates the conserved spacing of these residues within these motifs. Sequence coloring is based on ClustalX: light blue, hydrophobic and cysteine residues; purple, acids; green, bases; yellow, proline; and orange, glycine. MICALs contain a 100% match with the consensus ADP binding region of FAD binding proteins (FAD fingerprint 1), a well-conserved GD sequence (FAD fingerprint 2), and a well-conserved DG motif: distinguishing features of flavoprotein monooxygenases. The proline (asterisk) in the FAD fingerprint 2 is also likely to be conserved.

(B) MICAL is a FAD binding protein. A bacterial fusion protein consisting of the *Drosophila* MICAL flavoprotein monooxygenase (FM) domain has an absorption peak at 452 nm and a shoulder at ~358 nm, consistent with that of free FAD (red line) and similar in shape to spectra from other flavoproteins.

(C–H) The FAD binding region is necessary for MICAL function. Abdominal segments of filleted stage 16/17 embryos stained with mAb 1D4 to label motor axons within the ISNb and SNa are shown. Ventral muscles 6, 7, 12, and 13 and the intersegmental nerve (ISN) are shown. Anterior, left; dorsal, up.

(C) Neuronal expression of MICAL$^{G\rightarrow W}$ (see text) fails to rescue *MICAL* loss-of-function axon guidance defects. MICAL$^{G\rightarrow W}$ was expressed in all neurons in a *MICAL* LOF background and no rescue was seen of any *MICAL* motor or CNS pathfinding defects (e.g., ISNb [arrows]; fusion of ISNb axons with the ISN [arrowhead]).

(D–H) Overexpression of MICAL$^{G\rightarrow W}$ in all neurons in a wild-type background gives rise to highly penetrant axon guidance phenotypes that resemble *MICAL* LOF, GOF, and novel phenotypes not observed in *MICAL* mutants.

(D) ISNb (arrow) and SNa (arrowhead) phenotypes were consistent with, but often more severe than, *MICAL* LOF. In this segment, ISNb axons have fasciculated with the ISN and bypassed their muscle fields; however, at more dorsal regions some of these axons defasciculate from the ISN and then project into adjacent segments (arrows).

(E and F) ISNb and SNa phenotypes were consistent with, but often more severe than, *MICAL* GOF phenotypes. ISNb axons are severely defasciculated and tangled in this segment ([E], arrows and arrowheads), and SNa axons have projected in the wrong direction, into the wrong muscle fields, and across segment boundaries ([F], arrowheads).

(G and H) Phenotypes unlike *PlexA*, *Sema1a,* or *MICAL* LOF or GOF mutants.

(G) ISNb axons extend the entire length of the cleft between muscles 6 and 7 (arrowheads).

(H) SNa axons project abnormally across the ventral muscle fields and wander in circles (arrowheads, bottom) prior to defasciculating (arrows) and projecting dorsally where they appear to refasciculate in the vicinity of their correct pathways (arrowhead, top). Scale bar equals 24 μm (C) and 27 μm (D).

An Intact FAD Binding Motif Is Required for *MICAL* Motor Axon Guidance Functions

The glycine residues within the GXGXXG motif of FAD binding proteins are essential for allowing the FAD binding and enzymatic activity (Wierenga et al., 1986; Dym and Eisenberg, 2001). To test the necessity of MICAL FAD binding and potential enzymatic activity for plexin-mediated repulsive axon guidance, we mutated the three glycine residues within the FAD fingerprint 1 motif of MICAL to tryptophan (GAGPCGL→WAWPCWL). Similar mutations in related flavin-containing monooxygenases disrupt FAD binding but do not alter the overall structure of the protein (Kubo et al., 1997; Lawton and Philpot, 1993; Wierenga et al., 1986). The resulting construct, *MICAL*$^{G\rightarrow W}$, was used for in vivo neuronal expression in *Drosophila*. Transgenic flies containing the *UAS-MICAL*$^{G\rightarrow W}$ transgene were generated, and immunohistochemical and Western analyses confirmed that MICAL$^{G\rightarrow W}$ was expressed at levels comparable to those of our wild-type "short" MICAL variant that we used to rescue *MICAL* mutant motor axon guidance phenotypes (data not shown). Unlike neuronal expression of MICAL in a homozygous *Df(3R)swp2*^{MICAL} mutant background, which rescues all ISNb and SNa defects, one copy of the neuronal MICAL$^{G\rightarrow W}$ rescues none of these defects (e.g., Figure 6C; Table 1). This strongly suggests that activity of the MICAL monooxygenase domain is necessary for normal MICAL function.

Since MICAL$^{G\rightarrow W}$ contains an intact plexin-interacting domain but is functionally inactive, we predicted that it would exert a dominant-negative effect on motor axon projections in a wild-type genetic background, binding

to PlexA but blocking signaling in a manner similar to our MICAL$^{Myr\text{-}CT}$ construct. When one copy of the MICAL$^{G\rightarrow W}$ reporter construct was used to express MICAL$^{G\rightarrow W}$ in all neurons in a wild-type genetic background, we observed highly penetrant ISNb, SNa, and CNS longitudinal connective defects (Figures 6D–6H; Table 1; data not shown), providing further evidence that MICAL$^{G\rightarrow W}$ is being expressed neuronally and is likely able to bind PlexA. However, though many of these defects resemble phenotypes observed in *Sema1a*, *PlexA*, or *MICAL* LOF mutants (Table 1), a significant fraction (ISNb, >44%; SNa, 38%) were strikingly distinct (Table 1; Figures 6D–6H). For example, though we observed ISNb and SNa axon guidance phenotypes consistent with *MICAL* LOF phenotypes (Figure 6D; Table 1), these phenotypes were often more severe. They include defects in which axons bypass their muscle targets but then appear to defasciculate in inappropriate places and project into adjacent segments (e.g., Figure 6D). Interestingly, we also observed ISNb and SNa axon guidance phenotypes consistent with MICAL GOF, but these phenotypes also appeared more severe (e.g., Figures 6E and 6F) and included severely defasciculated and tangled axons (Figures 6E). Finally, we saw phenotypes unlike *MICAL* or *PlexA* LOF or GOF mutants, including axons projecting along the entire length of the muscle 6/7 cleft (Figure 6G) and dramatic axonal wandering within muscle fields (e.g., Figure 6H). These phenotypes suggest that expression of MICAL$^{G\rightarrow W}$ leads to defects not explained by a simple elevation or diminution of PlexA signaling activity.

In summary, these results show the necessity of an intact flavoprotein monooxygenase domain for MICAL function in repulsive motor axon guidance.

Flavoprotein Monooxygenase Inhibitors Neutralize Vertebrate Sema3A Axonal Repulsion

The MICALs may be susceptible to small molecule inhibitors that affect their ability to oxidize their substrate. Some gallic acid derivatives, including the green tea component (−)-epigallocatechin gallate (EGCG), are potent and selective inhibitors of two flavoprotein monooxygenases: squalene epoxidase (SE) and *p*-hydroxybenzoate hydroxylase (*p*HBH) (Abe et al., 2000a, 2000b).

All available evidence points to the plexin cytoplasmic domain as an essential signal-transducing domain for signaling class 3 semaphorin repulsion (Cheng et al., 2001; Takahashi and Strittmatter, 2001). Sema3A appears to utilize neuropilin-1 in combination with A class plexins to signal repulsive guidance. To ask whether selective flavoprotein monooxygenase inhibitors can neutralize semaphorin-mediated repulsion in vertebrates, we employed an in vitro rat DRG growth cone repulsion assay using Sema3A-secreting 293 cells (Figure 7A; Messersmith et al., 1995). NGF-dependent DRG axons exhibit little to no outgrowth toward Sema3A-secreting 293 cell aggregates (Figures 7C and 7G). However, when 25 μM EGCG is added to the growth media, Sema3A repulsion was completely neutralized (Figures 7D and 7G). EGCG attenuation of Sema3A-mediated repulsion is dose dependent (Figure 7G). We also asked whether (−)-epicatechin (EC), a compound structurally similar to EGCG but a poor inhibitor of SE (Abe et al., 2000b), had a similar effect on Sema3A-mediated repulsion. Like EGCG, EC was capable of completely neutralizing Sema3A-dependent repulsion in a dose-dependent manner, but a much higher EC concentration was required (Figures 7E and 7G). To address the possibility that a general inhibition of oxidation-reduction mechanisms by these reagents underlies this attenuation of Sema3A repulsion, we asked whether selective inhibitors of other redox enzymes present in neurons had any effect on Sema3A-mediated repulsion. We did not see attenuation of Sema3A-mediated axonal repulsion using inhibitors specific for nitric oxide synthase (N-nitro-L-arginine methylester [L-NAME]), xanthine oxidase (allopurinol [Allo]), or mitochondrial electron transport (NADH dehydrogenase; rotenone [Rote]) at concentrations previously shown to be effective in cell culture conditions (Figure 7G). DRG axons and Sema3A-secreting 293 cells appeared normal following growth in the presence of all but one of these inhibitors. In some explants we noticed an adverse effect on survival of DRGs treated with rotenone, but axons in those rotenone-treated explants that survived, although somewhat thinner than normal, were robustly repelled (Figure 7G). The amount and biological activity of Sema3A produced by 293 cells in the presence of all inhibitors was similar as assessed using a DRG growth cone collapse assay (Figure 7B), showing that none of these inhibitors had an adverse effect on the ability of 293 cells to produce active Sema3A. We also determined in separate experiments that 25 μM EGCG dramatically abrogates Sema3A-mediated growth cone collapse in NGF-dependent DRG neurons (Figure 7G). Taken together, our results support a role for flavoenzymes and oxidation-reduction mechanisms in semaphorin-mediated repulsive axon guidance.

Discussion

Neuronal growth cone guidance depends on the ability of various guidance cue receptors to regulate cytoskeletal dynamics in response to the local presentation of ligands. We show here that proteins belonging to the MICAL family of cytosolic, multidomain, flavoprotein monooxygenases are required for certain plexin-mediated semaphorin axon guidance events. MICALs associate with plexins and contain several conserved domains that provide the potential for interactions with both growth cone cytoskeletal components and many signaling proteins intimately involved in their regulation. Our results suggest that MICALs directly participate in plexin signaling through the action of their flavoprotein monooxygenase domain. These observations provide a framework for dissecting the molecular basis of semaphorin-meditated neuronal guidance and also a potential target for attenuating their repulsive action.

Our genetic and biochemical results support an essential role for *Drosophila* MICAL in mediating PlexA/Sema-1a repulsive guidance events required for motor axon pathfinding. Future experiments will establish whether MICAL mediates PlexB signaling, and if so, whether this occurs directly or indirectly. *Drosophila* MICAL is an ortholog of the previously characterized

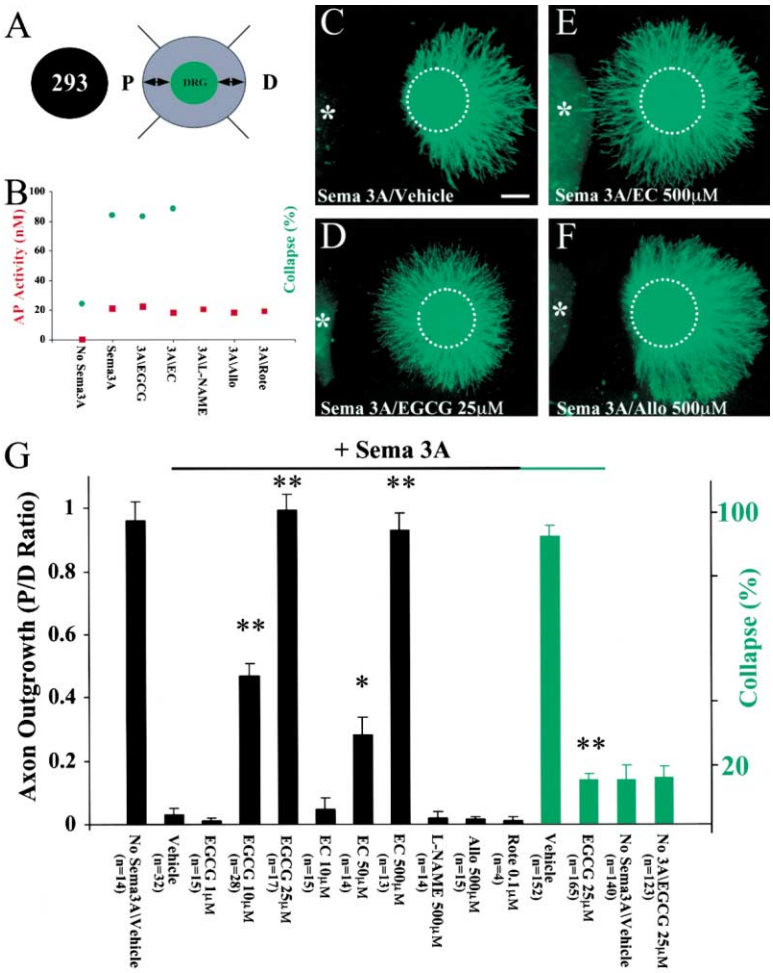

Figure 7. Flavoprotein Monooxygenase Inhibitors Attenuate Vertebrate Semaphorin Axonal Repulsion

Inhibitors of flavoprotein monooxygenases (EGCG and EC) as well as specific inhibitors of other oxidation/reduction enzymes including nitric oxide synthase (L-NAME), xanthine oxidase (allopurinol [Allo]), and mitochondrial electron transport (NADH dehydrogenase; rotenone [Rote]) were tested for their ability to inhibit semaphorin-dependent repulsive axon guidance in vertebrates.

(A) E14/15 Rat DRG explants were cocultured with 293 cells expressing Sema3A and grown for 48 hr in the presence of an inhibitor or vehicle. Axonal outgrowth was determined by measuring proximal (P) and distal (D) axon lengths.

(B) Redox inhibitors do not have adverse effects on expression of Sema3A or its biological activity. Media was collected from untransfected 293 cells (No Sema3A) or cells transfected with AP-Sema3A and grown in the presence of vehicle (Sema3A), 25 μM EGCG (3A/EGCG), 500 μM EC (3A/EC), 500 μM L-NAME (3A/L-NAME), 500 μM Allo (3A/Allo), or 0.1 μM Rote (3A/Rote), and ligand concentration (AP activity) was determined. The media was then diluted to 1 nM (to remove the active concentration of the inhibitor) and its biological activity was assayed in a growth cone collapse assay (percent collapse; $n > 60$ growth cones per condition). The AP activity and percentage of growth cones collapsed were similar in the presence of all compounds.

(C–F) Sema3A-secreting 293 cells (asterisk) potently repel DRG axons (C), but this effect is neutralized when DRG explants are grown in the presence of EGCG (D) or EC (E). No effect on repulsion was observed in the presence of Allo (F).

(G) Quantification of the effects of oxidation/reduction enzyme inhibitors on Sema3A repulsion scored as the ratio of the axon lengths on the proximal and distal sides of the explant (P/D ratio), and on Sema3A-mediated growth cone collapse indicated as percent collapsed growth cones (green). In repulsion assays, outgrowth of DRG axons on the side distal to the 293 cells appeared normal. Attenuation of Sema3A-mediated axonal repulsion was observed with the flavoprotein monooxygenase inhibitors (EGCG and EC) in a dose-dependent manner but not with specific inhibitors of other oxidation/reduction enzymes. n equals number of DRG explants (repulsion assays) or number of growth cones scored (collapse assays; distributed over four different explants/condition). For Rote, $n = 4$; however, only 4 out of 12 explants survived. (single asterisk indicates $p < 0.001$; double asterisk indicates $p < 0.0001$; paired t test). Scale bar equals 550 μm.

mammalian MICAL-1 protein (Suzuki et al., 2002), and we show here that there are at least three vertebrate MICAL orthologs (MICALs 1, 2, and 3). We also identify here a family of MICAL-like proteins that lack the conserved N-terminal MICAL monooxygenase domain. Our expression and interaction data support the idea that MICALs mediate plexin signaling in vertebrates. In addition, flavoprotein monooxygenase inhibitors block Sema3A-mediated repulsion and collapse of NGF-dependent DRG axons, repulsive interactions dependent on A class plexins including plexin A3. Future genetic and biochemical analysis will establish the role of vertebrate MICALs in neuronal and nonneuronal plexin signaling.

The highly conserved ~500 amino acid N-terminal MICAL domain contains signature amino acid sequences of the flavoprotein monooxygenase family of oxidoreductases. Our biochemical and genetic analyses strongly suggest that MICALs contain functional FAD binding monooxygenase domains required for mediating plexin signaling. In support of this idea, we observed that inhibition of flavoprotein monooxygenase enzymatic activity dramatically attenuates semaphorin-mediated axon repulsion and growth cone collapse. However, though the inhibitor EGCG has a high degree of selectivity for flavoprotein monooxygenases, similar concentrations of EGCG inhibit other enzymes including steroid 5α-reductase, NADPH-cytochrome P450 reductase, telomerase, matrix metalloproteinases MMP-2 and MMP-9, and phenol sulfotransferase (Abe et al., 2000a, 2000b). Although most of these enzymes are unlikely to be expressed in the growth cones of DRG axons, we cannot rule out potential nonspecific effects of these inhibitors despite their demonstrated selectivity for monooxygenases. Taken together with our in vivo *Drosophila* experiments showing a requirement for the MICAL FAD binding region in Sema-1a-mediated axon repulsion, these data suggest redox signaling plays an

important role in vertebrate semaphorin-mediated axonal repulsion.

Flavoprotein monooxygenases specifically catalyze the oxidation of a number of substrates, and in some contexts they can function as oxidases and generate reactive oxygen species (Massey, 1994). Our results suggest that MICALs are flavoproteins most similar to the flavoprotein monooxygenase family of oxidoreductases, but a complete understanding of the chemical nature of the reactions catalyzed by MICALs awaits future study and identification of substrates. The redox regulation of amino acid residues within signaling proteins (including kinases, phosphatases, small GTPases, guanylate cyclases, and adaptor proteins) and cytoskeletal proteins (including actin, actin binding proteins, intermediate filament proteins, and GAP-43) has been shown to modulate their function (Finkel, 1998; Kim et al., 2002; Meng et al., 2002; Rhee et al., 2000; Stamler et al., 2001; Thannickal and Fanburg, 2000). In addition, oxidation of actin leads to disassembly of actin filaments, instability and collapse of actin networks, reduced ability of actin to interact with actin crosslinking proteins, and a decrease in the ability of actin monomers to form polymers (Dalle-Donne et al., 2001a, 2001b; Milzani et al., 1997). Finally, it is also interesting that MICALs have a putative actin filament binding domain (CH domain) and that MICAL-1 interacts with vimentin, an intermediate filament protein (Suzuki et al., 2002).

It was recently reported that the proline-rich region of vertebrate MICAL-1 interacts with the SH3 domain of the adaptor protein CasL (HEF1) in nonneuronal cells (Suzuki et al., 2002). CasL, along with the related proteins p130Cas and Efs (Sin), make up the Cas family of proteins (O'Neill et al., 2000), which assemble and transduce intracellular signals that stimulate cell migration and axon outgrowth. These proteins have numerous protein-protein interaction domains, including a Src-homology 3 (SH3) domain, multiple SH2 binding sites in their substrate domain, several proline-rich motifs, and a C-terminal dimerization module. This structure suggests a role for Cas family proteins as docking molecules, and numerous interacting proteins have been identified, including kinases (e.g., FAK, Src, and Abl), phosphatases (e.g., PTP-1B and SHP2), GEFs (e.g., C3G), and adaptor proteins (e.g., Nck, Crk, Grb2, and 14-3-3) (O'Neill et al., 2000). Studies indicate that Cas proteins localize mainly to focal adhesions and stress fibers and that they are required in integrin-dependent cell migration and actin filament assembly. Cas proteins, therefore, may play an important role in plexin-mediated repulsive and attractive guidance events.

In conclusion, we have characterized a gene family, conserved from invertebrates to vertebrates, with proteins whose structure and function strongly suggest that redox signaling is important for semaphorin-mediated axonal repulsion. Our results also suggest that protein oxidation could be a general means for inhibiting axonal growth. Given the presence of high amounts of reactive oxygen species and other oxidants in the spinal cord after injury (Juurlink and Paterson, 1998), regulation of redox signaling using antioxidants and specific enzyme inhibitors may be a powerful approach for encouraging axonal regeneration.

Experimental Procedures

Yeast Two-Hybrid Screening

Yeast protocols were conducted using standard techniques (Golemis et al., 1994). Portions of the intracellular domains of PlexA (amino acids 1702–1945; EST LD13083), PlexB (amino acids 1785–2051; EST CK00213), and the corresponding intracellular regions of human Plexin A3 and mouse Plexin A4 (gifts of L. Tamagnone and H. Fujisawa, respectively) were inserted into the yeast bait vector. cDNAs containing the C-terminal of human MICAL-1 (DFkzp434B517) and mouse MICAL-2 (BB481898) were used to amplify portions homologous to the last 200 amino acids of *Drosophila* MICAL and cloned into the library vector.

Molecular Analysis

Proteins, domains, and alignments were identified using Web-based protein domain searching and alignment tools (PFAM, BLAST, PRINTS, JALVIEW, and ClustalX) and our own molecular analysis. Human *MICAL-1* (EST FLJ11937), human *MICAL-2* (ESTs KIAA0750 and FLJ14966), and human *MICAL-3* (ESTs BF815128, KIAA1364, and KIAA0819) were identified by BLAST searches on publicly available cDNA, and genomic sequence and in some cases overlapping ESTs were assembled virtually. *Drosophila MICAL-L* (EST LD45758) and human *MICAL-L1* (EST XM001070) and *MICAL-L2* (ESTS FL00139 and FLJ23471) were identified by searching publicly available cDNA and genomic sequence databases.

In Situ Hybridization

RNA in situ analysis of whole-mount *Drosophila* embryos and cryosections of E15 and E18 rat spinal cords were as described (Kolodkin et al., 1993; Pasterkamp et al., 1998).

MICAL Antibody Generation, Western Analysis, Immunohistochemistry, and Immunoprecipitation

Antibodies were generated and characterized as described (Yu et al., 1998). cDNAs corresponding to the last 359 aa of MICAL (MICAL-CT antibody) were inserted into the pTrcHisA vector (Invitrogen). MICAL-CT antibodies were used for Western analysis at a 1:2000 dilution and on *Drosophila* embryos at a 1:3000 dilution.

Embryos generated by crossing UAS-HAPlexA and Elav-GAL4/Cyo adults were collected, and coimmunoprecipitations were performed using standard techniques (see Supplemental Data at http://www.cell.com/cgi/content/full/109/7/887/DC1) and an HA monoclonal antibody (12CA5; Roche). Western analysis was performed using an HA antibody (1:3000, rat mAb Clone 3F10, Roche), our MICAL-CT antibody (1:2000), and an Enabled antibody (1:500; IG6C10; gift from D. VanVactor).

Drosophila Genetics and Phenotypic Characterization

Drosophila genetics, transformations, and preparation and analyses of *Drosophila* embryos was performed as described (Winberg et al., 1998b; Yu et al., 1998; see Supplemental Data at http://www.cell.com/cgi/content/full/109/7/887/DC1).

Vertebrate In Vitro Repulsion and Collapse Assays

DRG repulsion assays were performed as described (Messersmith et al., 1995). EGCG, EC, L-NAME, and allopurinol (Sigma) were dissolved in vehicle (PBS), protected from light, and then added to the culture media to final concentrations. Rotenone (Sigma) was dissolved in 95% EtOH and then added to the culture media (final EtOH concentration was below 0.1% and had no effect on axon outgrowth) (see Supplemental Data).

MICAL Flavoprotein Monooxygenase Fusion Protein Purification and FAD Binding

His-tagged bacterial fusion protein comprised of the MICAL flavoprotein monooxygenase domain (MICAL-FM) was made by inserting amino acids 1–526 of *Drosophila* MICAL into the bacterial expression vector pET 43.1b (Novagen). MICAL-FM was isolated with the inclusion bodies, denatured with 6 M GdmHCl (GIBCO), and purified under denaturing conditions over a Ni^{2+} column (Novagen). MICAL-FM was renatured as described (Lindsay et al., 2000; see Supplemental Data) and repurified over a Ni^{2+} column. Spectral analysis

was done using a Perkin-Elmer UV/VIS Lambda-35 spectrophotometer scanning from 300 to 550 nm.

Acknowledgments

We especially thank Y.-C. Wu for *Drosophila* technical assistance, N. Schumann and S. Kohli for help with yeast interaction assays, and C. Foster for help with MICAL-FM purification and analysis. We thank A. Ghosh, D. Ginty, and H. Sink for helpful comments on the manuscript, and M. Amzel, K. Cook, C. Foster, M. Grimes, and members of the Kolodkin and Ginty laboratories for helpful discussions. We thank M. Ashburner, H. Araj, C. Goodman, H. Fujisawa, T. Nagase, J. Roote, L. Tamagnone, D. VanVactor, K. Zinn, the Bloomington Stock Center, and the Berkeley Drosophila Genome Project for cDNA libraries, fly stocks, antibodies, and cDNAs. Supported by National Institutes of Health (NRSA-NS11055) and The Paralyzed Veterans Association of America/Spinal Cord Research Foundation (#2050) (J.R.T), the Netherlands Organization for Scientific Research and Human Frontier Science Organization (R.J.P.), and NIH grant NS35165 (A.L.K.).

Received: May 20, 2002
Revised: June 7, 2002
Published online: June 14, 2002

References

Abe, I., Kashiwagi, K., and Noguchi, H. (2000a). Antioxidative galloyl esters as enzyme inhibitors of p-hydroxybenzoate hydroxylase. FEBS Lett. *483*, 131–134.

Abe, I., Seki, T., Umehara, K., Miyase, T., Noguchi, H., Sakakibara, J., and Ono, T. (2000b). Green tea polyphenols: novel and potent inhibitors of squalene epoxidase. Biochem. Biophys. Res. Commun. *268*, 767–771.

Bach, I. (2000). The LIM domain: regulation by association. Mech. Dev. *91*, 5–17.

Brand, A.H., and Perrimon, N. (1993). Targeted gene expression as a means of altering cell fates and generating dominant phenotypes. Development *118*, 401–415.

Bretscher, A., Chambers, D., Nguyen, R., and Reczek, D. (2000). ERM-Merlin and EBP50 protein families in plasma membrane organization and function. Annu. Rev. Cell Dev. Biol. *16*, 113–143.

Cheng, H.J., Bagri, A., Yaron, A., Stein, E., Pleasure, S.J., and Tessier-Lavigne, M. (2001). Plexin-A3 mediates semaphorin signaling and regulates the development of hippocampal axonal projections. Neuron *32*, 249–263.

Dalle-Donne, I., Rossi, R., Giustarini, D., Gagliano, N., Lusini, L., Milzani, A., Di Simplicio, P., and Colombo, R. (2001a). Actin carbonylation: from a simple marker of protein oxidation to relevant signs of severe functional impairment. Free Radic. Biol. Med. *31*, 1075–1083.

Dalle-Donne, I., Rossi, R., Milzani, A., Di Simplicio, P., and Colombo, R. (2001b). The actin cytoskeleton response to oxidants: from small heat shock protein phosphorylation to changes in the redox state of actin itself. Free Radic. Biol. Med. *31*, 1624–1632.

Dym, O., and Eisenberg, D. (2001). Sequence-structure analysis of FAD-containing proteins. Protein Sci. *10*, 1712–1728.

Eggink, G., Engel, H., Vriend, G., Terpstra, P., and Witholt, B. (1990). Rubredoxin reductase of *Pseudomonas oleovorans*. Structural relationship to other flavoprotein oxidoreductases based on one NAD and two FAD fingerprints. J. Mol. Biol. *212*, 135–142.

Eppink, M.H., Schreuder, H.A., and Van Berkel, W.J. (1997). Identification of a novel conserved sequence motif in flavoprotein hydroxylases with a putative dual function in FAD/NAD(P)H binding. Protein Sci. *6*, 2454–2458.

Fan, J., Mansfield, S.G., Redman, T., Phillip, R., Gordon-Weeks, P.R., and Raper, J.A. (1993). The organization of F-actin and microtubules in growth cones exposed to a brain-derived collapsing factor. J. Cell Biol. *121*, 867–878.

Finkel, T. (1998). Oxygen radicals and signaling. Curr. Opin. Cell Biol. *10*, 248–253.

Gimona, M., Djinovic-Carugo, K., Kranewitter, W.J., and Winder, S.J. (2002). Functional plasticity of CH domains. FEBS Lett. *513*, 98–106.

Golemis, E.A., Gyuris, J., and Brent, R. (1994). Interaction trap/two hybrid system to identify interacting proteins. In Current Protocols in Molecular Biology (New York: Wiley), pp. 13.14.1–13.14.17.

Harris, B.Z., and Lim, W.A. (2001). Mechanism and role of PDZ domains in signaling complex assembly. J. Cell Sci. *114*, 3219–3231.

He, Z., Wang, K.C., Koprivica, V., Ming, G., and Song, H.J. (2002). Knowing how to navigate: mechanisms of semaphorin signaling in the nervous system. Sci STKE *119*, RE1.

Hosokawa, K., and Stanier, R.Y. (1966). Crystallization and properties of p-hydroxybenzoate hydroxylase from *Pseudomonas putida*. J. Biol. Chem. *241*, 2453–2460.

Juurlink, B.H., and Paterson, P.G. (1998). Review of oxidative stress in brain and spinal cord injury: suggestions for pharmacological and nutritional management strategies. J. Spinal Cord Med. *21*, 309–334.

Kim, S.O., Merchant, K., Nudelman, R., Beyer, W.F., Keng, T., DeAngelo, J., Hausladen, A., and Stamler, J.S. (2002). OxyR: a molecular code for redox-related signaling. Cell *109*, 383–396.

Kolodkin, A.L., Matthes, D., and Goodman, C.S. (1993). The semaphorin genes encode a family of transmembrane and secreted growth cone guidance molecules. Cell *75*, 1389–1399.

Kubo, A., Itoh, S., Itoh, K., and Kamataki, T. (1997). Determination of FAD-binding domain in flavin-containing monooxygenase 1 (FMO1). Arch. Biochem. Biophys. *345*, 271–277.

Landgraf, M., Bossing, T., Technau, G.M., and Bate, M. (1997). The origin, location, and projections of the embryonic abdominal motorneurons of *Drosophila*. J. Neurosci. *17*, 9642–9655.

Lawton, M.P., and Philpot, R.M. (1993). Functional characterization of flavin-containing monooxygenase 1B1 expressed in *Saccharomyces cerevisiae* and *Escherichia coli* and analysis of proposed FAD- and membrane-binding domains. J. Biol. Chem. *268*, 5728–5734.

Lindsay, H., Beaumont, E., Richards, S.D., Kelly, S.M., Sanderson, S.J., Price, N.C., and Lindsay, J.G. (2000). FAD insertion is essential for attaining the assembly competence of the dihydrolipoamide dehydrogenase (E3) monomer from *Escherichia coli*. J. Biol. Chem. *275*, 36665–36670.

Liu, B.P., and Strittmatter, S.M. (2001). Semaphorin-mediated axonal guidance via Rho-related G proteins. Curr. Opin. Cell Biol. *13*, 619–626.

Macheroux, P. (1999). UV-visible spectroscopy as a tool to study flavoproteins. Methods Mol. Biol. *131*, 1–7.

Massey, V. (1994). Activation of molecular oxygen by flavins and flavoproteins. J. Biol. Chem. *269*, 22459–22462.

Massey, V. (1995). Introduction: flavoprotein structure and mechanism. FASEB J. *9*, 473–475.

Matthes, D.J., Sink, H., Kolodkin, A.L., and Goodman, C.S. (1995). Semaphorin II can function as a selective inhibitor of specific synaptic arborizations in *Drosophila*. Cell *81*, 631–639.

Meng, T.C., Fukada, T., and Tonks, N.K. (2002). Reversible oxidation and inactivation of protein tyrosine phosphatases in vivo. Mol. Cell *9*, 387–399.

Messersmith, E.K., Leonardo, E.D., Shatz, C.J., Tessier-Lavigne, M., Goodman, C.S., and Kolodkin, A.L. (1995). Semaphorin III can function as a selective chemorepellent to pattern sensory projections in the spinal cord. Neuron *14*, 949–959.

Milzani, A., Dalle-Donne, I., and Colombo, R. (1997). Prolonged oxidative stress on actin. Arch. Biochem. Biophys. *339*, 267–274.

O'Neill, G.M., Fashena, S.J., and Golemis, E.A. (2000). Integrin signalling: a new Cas(t) of characters enters the stage. Trends Cell Biol. *10*, 111–119.

Pasterkamp, R.J., De Winter, F., Holtmaat, A.J.G.D., and Verhaagen, J. (1998). Evidence for a role of the chemorepellent semaphorin III and its receptor neuropilin-1 in the regeneration of primary olfactory axons. J. Neurosci. *18*, 9962–9976.

Raper, J.A. (2000). Semaphorins and their receptors in vertebrates and invertebrates. Curr. Opin. Neurobiol. *10*, 88–94.

Rhee, S.G., Bae, Y.S., Lee, S.R., and Kwon, J. (2000). Hydrogen peroxide: a key messenger that modulates protein phosphorylation through cysteine oxidation. Sci STKE *53*, PE1.

Schulz, G.E. (1992). Binding of nucleotides by proteins. Curr. Opin. Struct. Biol. *2*, 61–67.

Semaphorin Nomenclature Committee. (1999). Unified nomenclature for the semaphorins/collapsins. Cell *97*, 551–552.

Stamler, J.S., Lamas, S., and Fang, F.C. (2001). Nitrosylation: the prototypic redox-based signaling mechanism. Cell *106*, 675–683.

Suzuki, T., Nakamoto, T., Ogawa, S., Seo, S., Matsumura, T., Tachibana, K., Morimoto, C., and Hirai, H. (2002). MICAL, a novel CasL interacting molecule, associates with vimentin. J. Biol. Chem. *277*, 14933–14941.

Takahashi, T., and Strittmatter, S.M. (2001). PlexinA1 autoinhibition by the plexin Sema domain. Neuron *29*, 429–439.

Tamagnone, L., and Comoglio, P.M. (2000). Signalling by semaphorin receptors: cell guidance and beyond. Trends Cell Biol. *10*, 377–383.

Thannickal, V.J., and Fanburg, B.L. (2000). Reactive oxygen species in cell signaling. Am. J. Physiol. Lung Cell. Mol. Physiol. *279*, L1005–L1028.

Vallon, O. (2000). New sequence motifs in flavoproteins: evidence for common ancestry and tools to predict structure. Proteins *38*, 95–114.

VanVactor, D., Sink, H., Fambrough, D., Tsoo, R., and Goodman, C.S. (1993). Genes that control neuromuscular specificity in *Drosophila*. Cell *73*, 1137–1153.

White, D.J., Merod, R., Thomasson, B., and Hartzell, P.L. (2001). GidA is an FAD-binding protein involved in development of *Myxococcus xanthus*. Mol. Microbiol. *42*, 503–517.

Whitford, K.L., and Ghosh, A. (2001). Plexin signaling via off-track and rho family GTPases. Neuron *32*, 1–3.

Wierenga, R.K., Terpstra, P., and Hol, W.G. (1986). Prediction of the occurrence of the ADP-binding beta alpha beta-fold in proteins, using an amino acid sequence fingerprint. J. Mol. Biol. *187*, 101–107.

Winberg, M.L., Mitchell, K.J., and Goodman, C.S. (1998a). Genetic analysis of the mechanisms controlling target selection: complementary and combinatorial functions of netrins, semaphorins, and IgCAMs. Cell *93*, 581–591.

Winberg, M.L., Noordermeer, J.N., Tamagnone, L., Comoglio, P.M., Spriggs, M.K., Tessier-Lavigne, M., and Goodman, C.S. (1998b). Plexin A is a neuronal semaphorin receptor that controls axon guidance. Cell *95*, 903–916.

Xu, X.M., Fisher, D.A., Zhou, L., White, F.A., Ng, S., Snider, W.D., and Luo, Y. (2000). The transmembrane protein semaphorin 6A repels embryonic sympathetic axons. J. Neurosci. *20*, 2638–2648.

Yu, H.H., Araj, H.H., Ralls, S.A., and Kolodkin, A.L. (1998). The transmembrane semaphorin Sema I is required in *Drosophila* for embryonic motor and CNS axon guidance. Neuron *20*, 207–220.

Accession Numbers

The GenBank accession numbers are as follows: D-MICAL (short), AF520713; D-MICAL (medium), AF520714; D-MICAL (long), AF520715; D-MICAL-L, AF520716; H-MICAL-2, BK000462, BK000463; H-MICAL-3, BK000464, BK000465; H-MICAL-L1, BK000466; and H-MICAL-L2, BK000467.